COnCOrD – Journées annuelles 2025
UTT TYroyes

Oxidation Resistance of High Entropy Nitride Thin Films Deposited by Magnetron Sputtering

A. BOUISSIL, D. TOUAIBIA, B. PANICAUD, M. EL GARAH, F. SANCHETTE,

LASMIS, Antenne de Nogent – LRC CEA-LASMIS, Nogent International Center for Coating Innovation (NICCI)
52, Pôle Technologique de Sud – Champagne, 52800 Nogent, France.

Content:

INTRODUCTION

- Deposition / target poisoning

- Structure / μstructure / Morphology

- Mechanical properties.

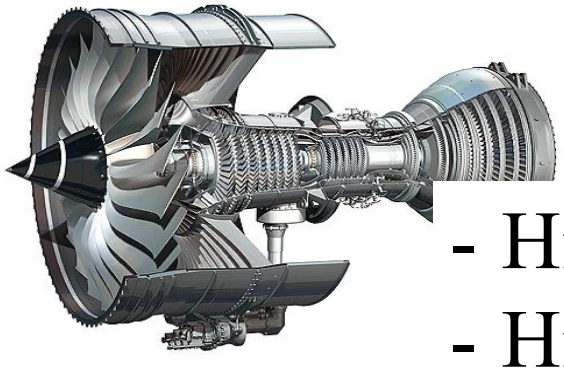
- High temperature oxidation resistance.

- Effect of Si addition on the oxidation resistance.

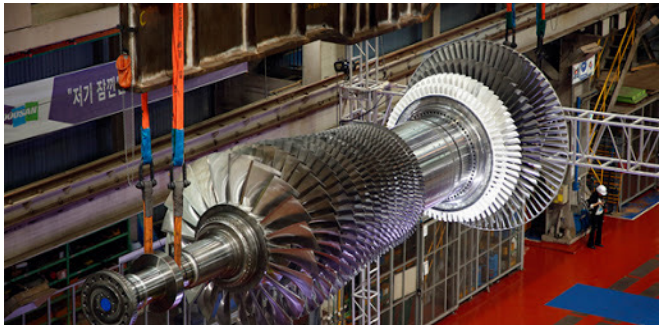
CONCLUSION.

The French Alternative Energies and Atomic Energy Commission (CEA)

New technologies for Transports, Energies



Aerospace gas turbin engines



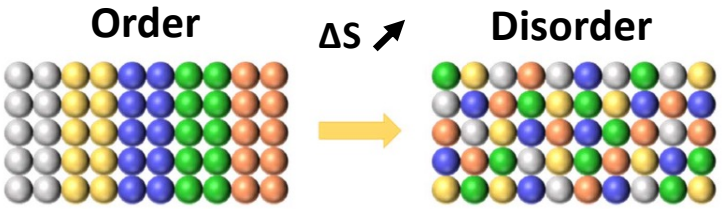


- High mechanical properties
- High ductility
- Good thermal stability
- Good oxidation resistance at high températures

Mate
chem
in se

re

INTRODUCTION



- Deposition of alloys with 5 metallic elements by means of an out of thermodynamic equilibrium technology (MS)
- FCC single phased materials

High entropy alloy

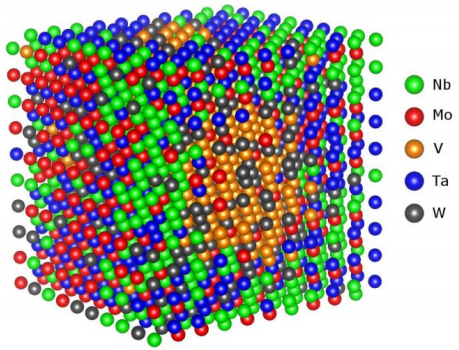
=

Alloy of at least 5 elements

+

atomic [element] between 5 and 35at.%

Ta-Zr-Hf-Ti-(Al/W) (-N) thin films



HEA features:

1- ΔS ↗

2- D ↘ → Sluggish diffusion.

⇒ Phase stability at T ↗.

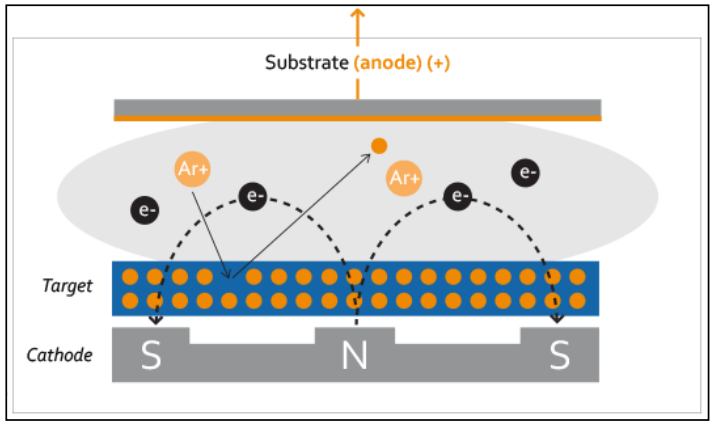
3- Lattice distortion.

4- Cocktail effect. ……..[Yeh].

EJ. Yeh, S et al. **Adv. Eng. Mater., 6 (2004), pp. 299-303**

Deposition / target poisoning

Powder metallurgically prepared target of equimolar Ta, Ti, Zr, Hf and Al/W mixture.



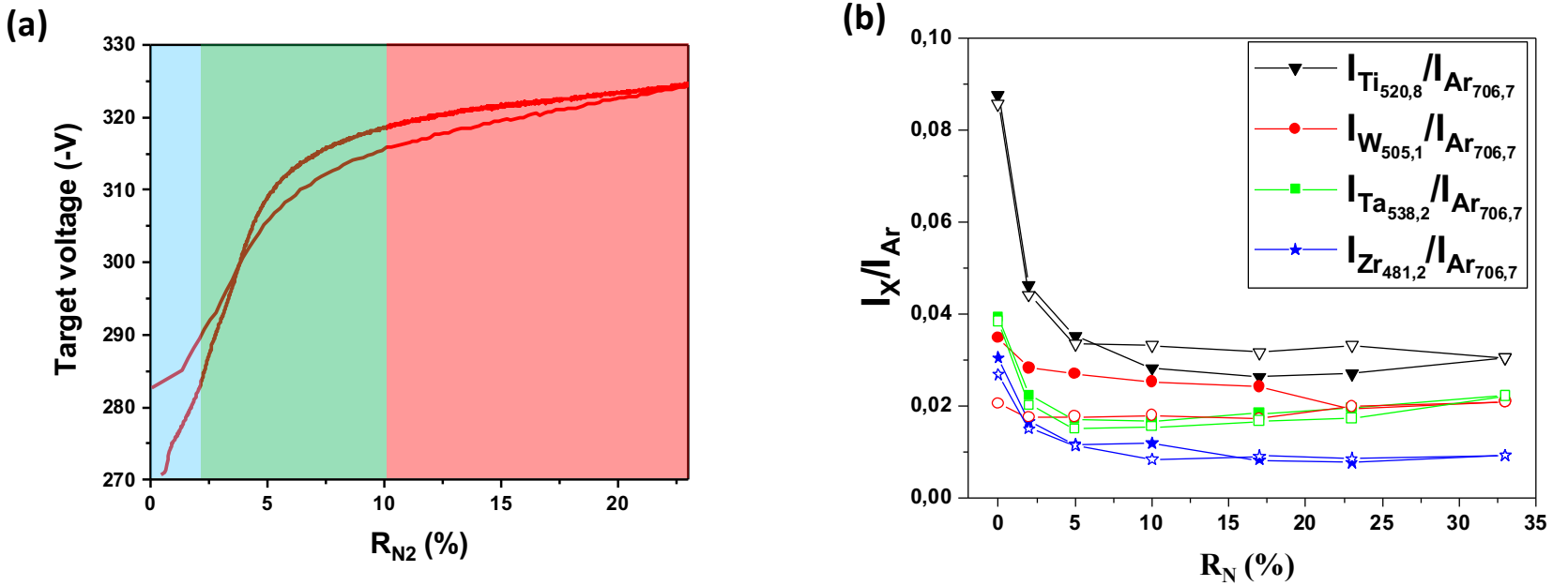
Magnetron sputtering.

Deposition parameters			
I (A)	P (Pa)	$R_{N2}=\Phi_{N2}/\Phi_{N2}+\Phi_{Ar}$	Mode / Rpm
1 ($3.2\ 10^{-3}$ A/cm^2)	1	[0% - 50%]	Dynamic (sweep) / 2 Rpm

- Equi-atomic target: Al/W, Ti, Zr, Ta and Hf.
- Target – substrate distance = 6 cm.

Deposition / target poisoning

OES

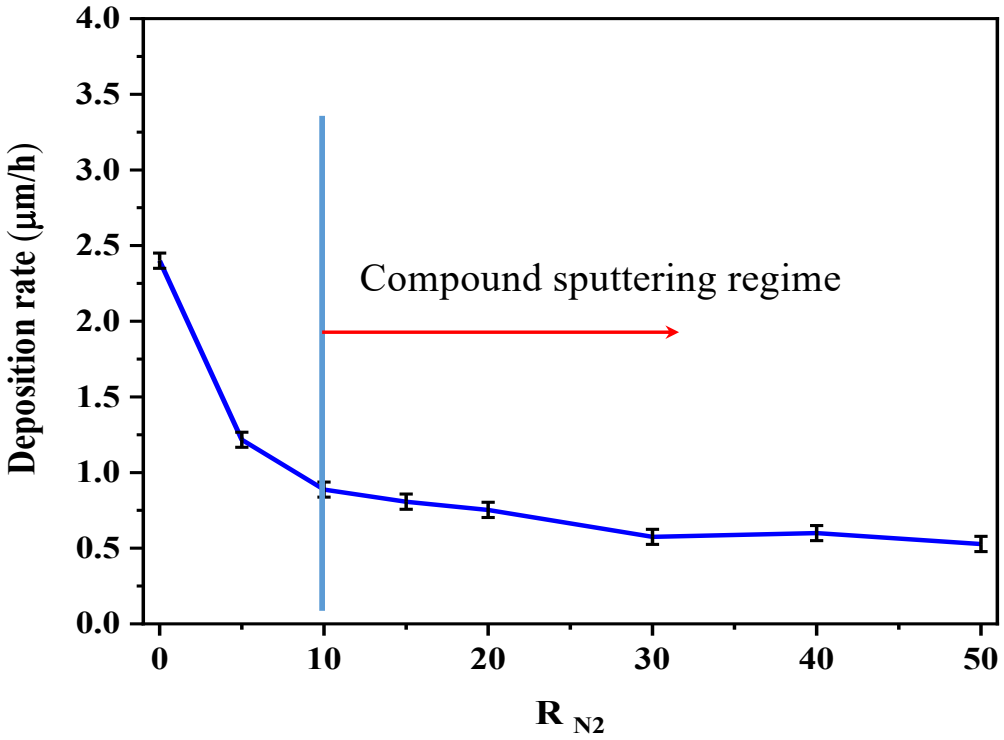


Target voltage (a) and normalized target species characteristic's emission lines intensities (b) as a function of R_{N2}

- First domain
  - The discharge voltage is stable.
  - The saturations of the emission lines of the metallic elements on the emission line of argon decrease.
- Second domain
  - the target begins to be poisoned by nitrogen.
  - The stabilization of the density of the metal species in the plasma is also observed.
  - It is the transition from the metal sputtering regime to the compound sputtering regime.
- the walls of the reactor become saturated and a nitride layer grows on the target surface

Deposition / target poisoning

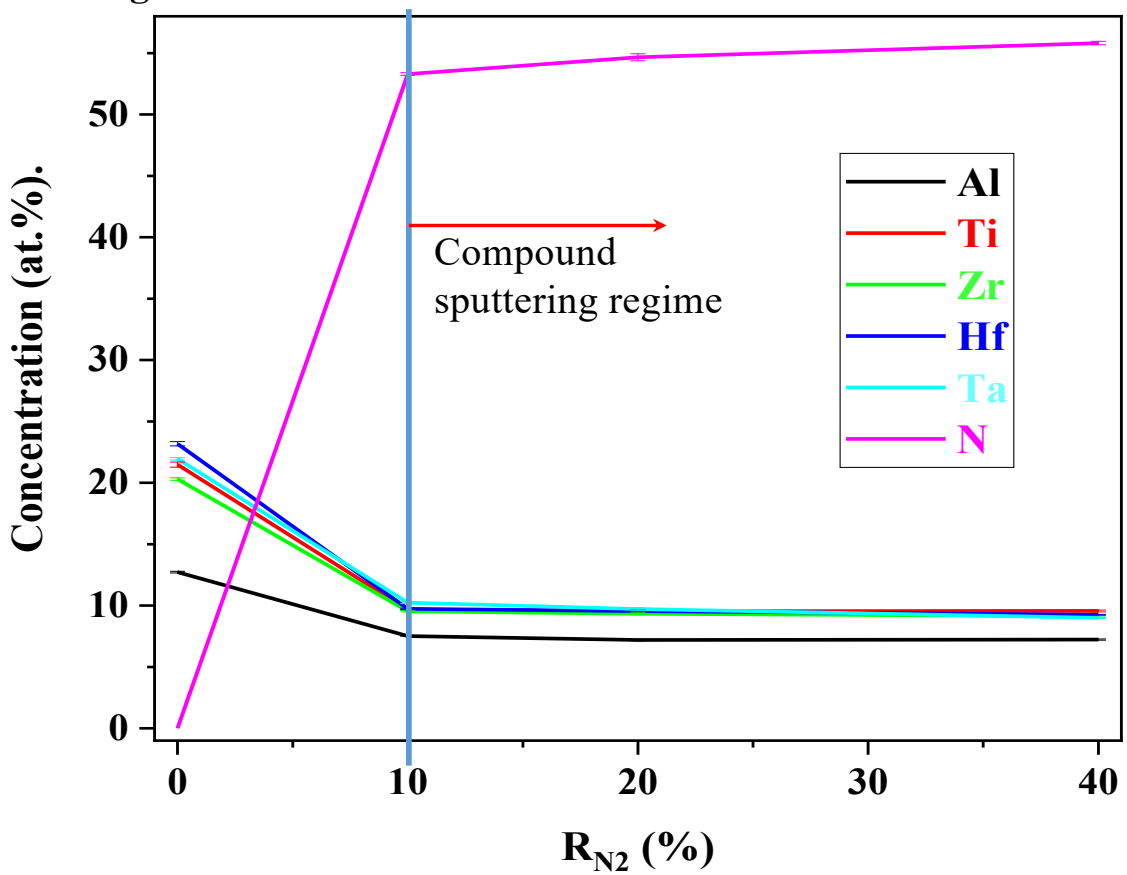
Deposition rate:



Ta-Zr-Hf-Ti-(Al) (-N) high entropy films

- When the nitrogen is introduced in the gas mixture, the deposition rate is decreased.
- $R_{N2} \geq 30\%$, the deposition rate is quite constant due to the complete target poisoning

Deposition / target poisoning

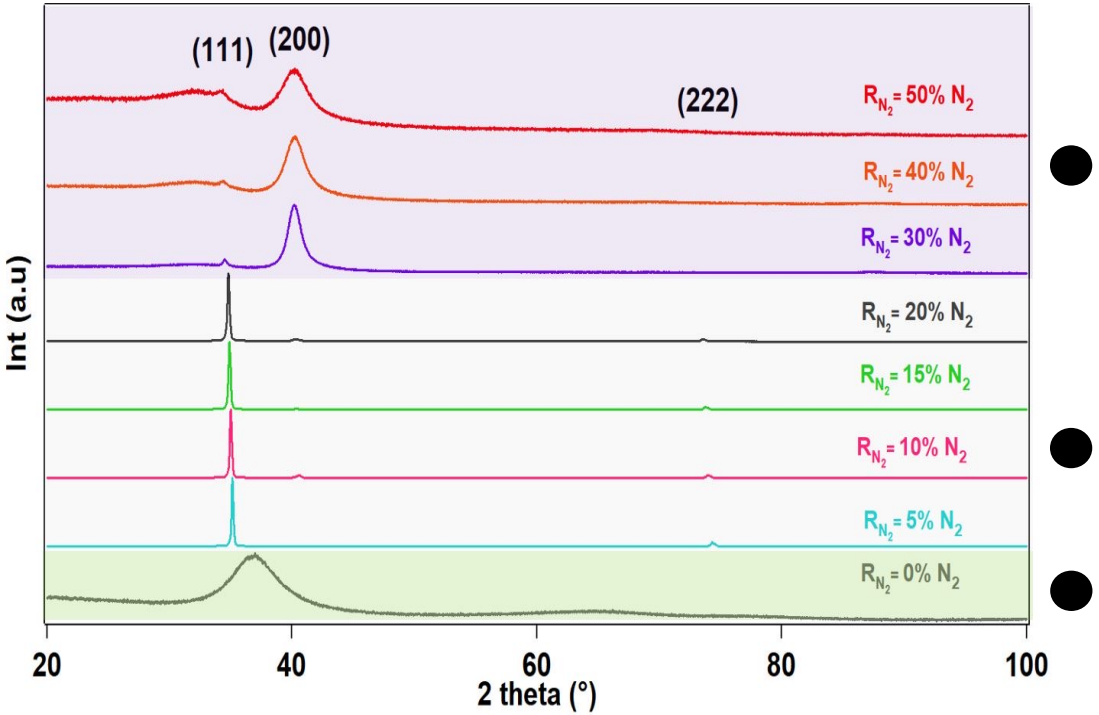


Chemical composition of Ta-Zr-Hf-Ti-(Al) (-N) high entropy films as a function of R_{N2}(EPMA Analysis).

- When the nitrogen is introduced the metal content is decreased.
- $R_{N2} \geq 10\%$, a stoichiometric composition is reached.

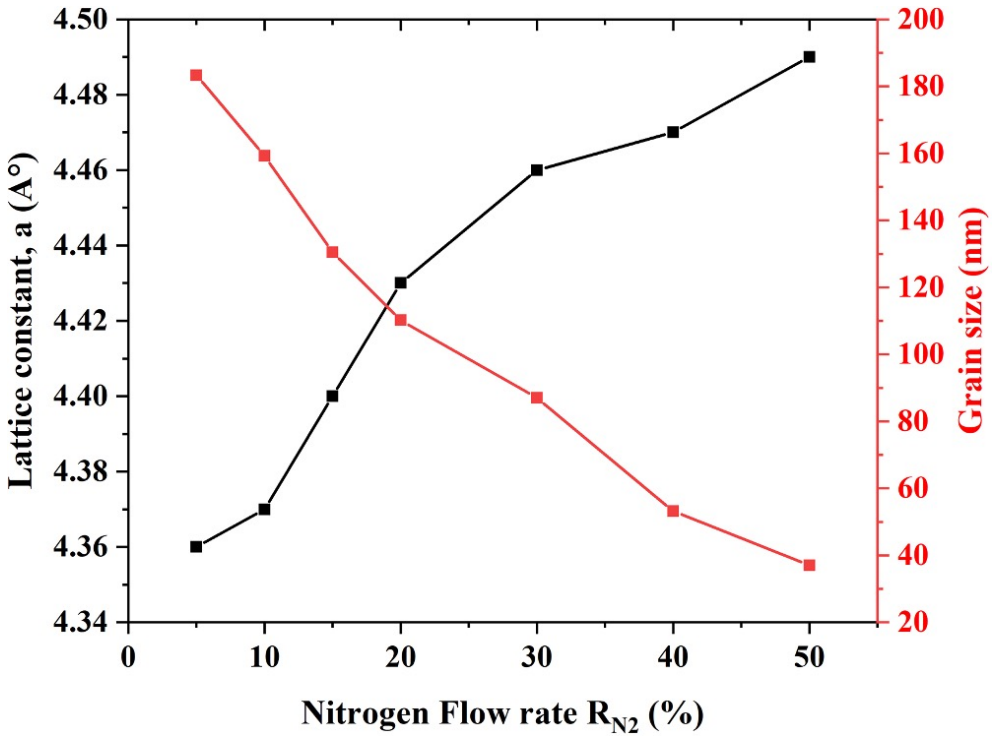
Structure / µstructure/ Morphology

Diffractograms of Ta-Zr-Hf-Ti-(Al) (-N) high entropy films as a function of R_{N2}.



- The film obtained at R_{N2} = 0% seems to be amorphous single phased (high mixing entropy and large atomic size mismatch).
- The increase of nitrogen flow R_{N2} > 0% leads to the formation of a FCC single-phased solid solution (FCC-NaCl type).
- Up to R_{N2} = 20%, an out of plan {111} preferential orientation is observed for all nitrides. For $R_{N2} \geq 30\%$, a change to {200} orientation is highlighted, probably due to the increasing N/Metal atomic flows ratio.

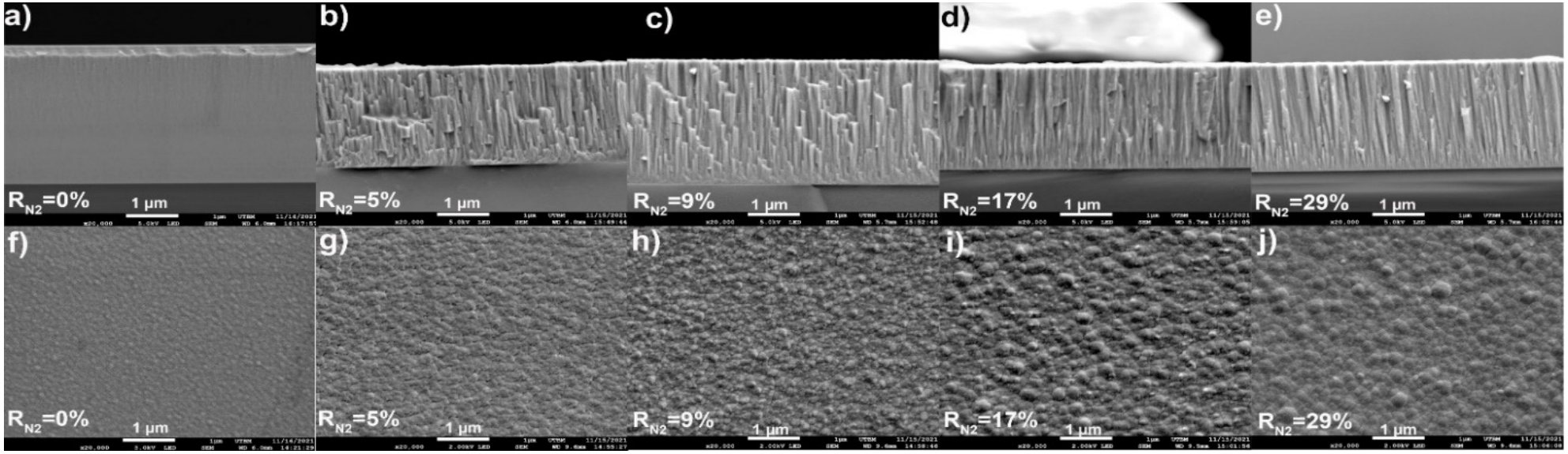
Structure / µstructure/ Morphology



A slight increase in the lattice parameter as a function of RN_2. This increase may be related to stress associated with interstitial atoms trapped in the lattice.

The mean grain size decreases when RN_2 increases from 5% to 50%. This phenomenon is well known in metalloid-enriched thin films.

Ta-Zr-Hf-Ti-(W) (-N) high entropy films

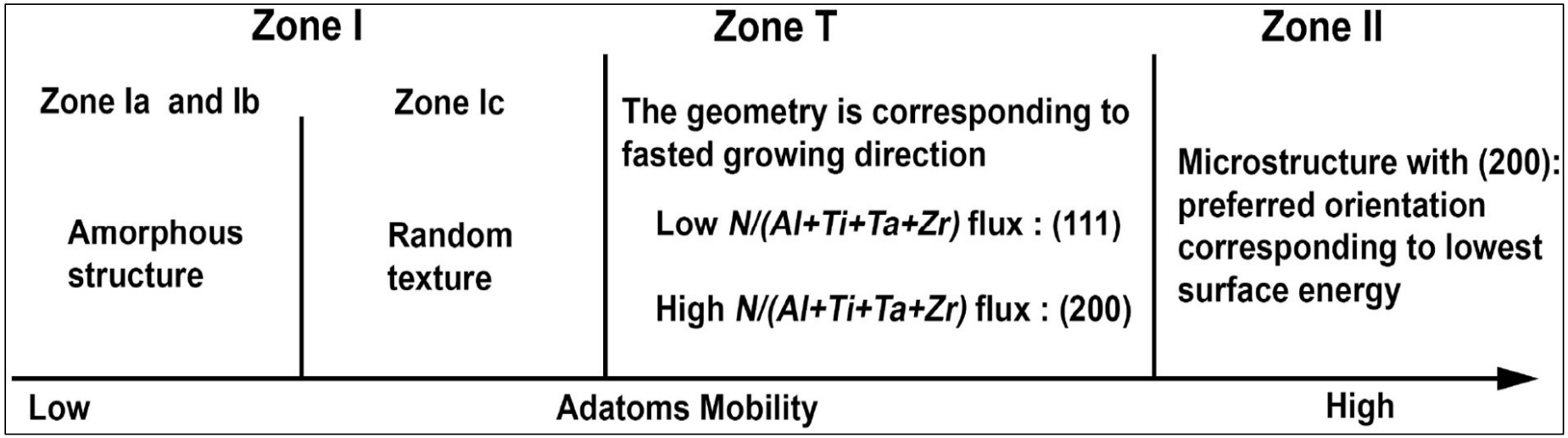


Cross-sectional and plan view SEM images of Ta-Zr-Hf-Ti-(W) (-N) films as a function of R_N.

- Metallic film presents a compact/glassy morphology associated with the amorphous structure.
- Concerning nitride films ($R_{N2} \geq 5\%$), a columnar growth is observed with a growing large lateral size as R_{N2} increases.

  → growth type corresponds to the zone T of the structure zone model (SZMs)

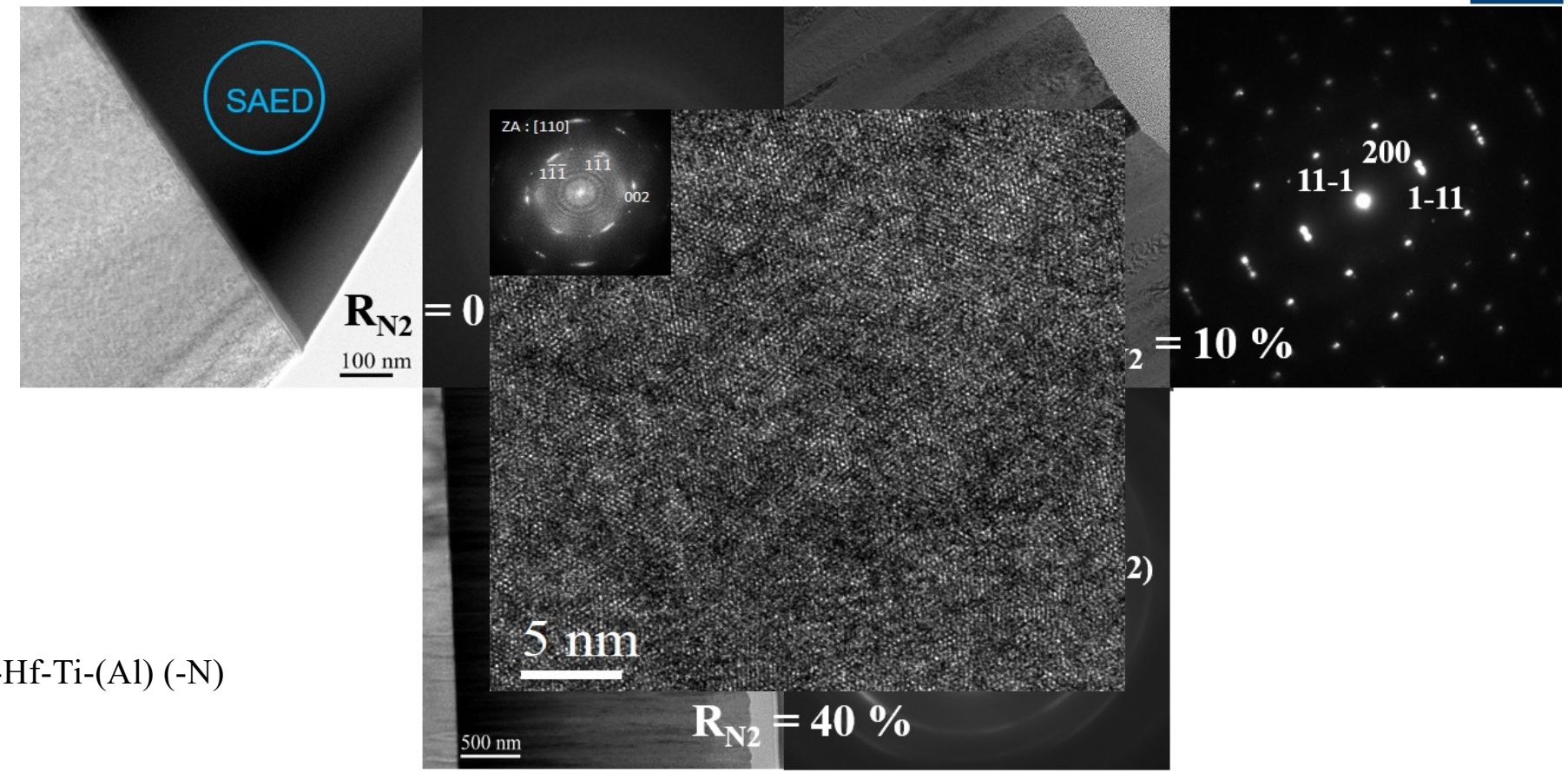
S. Mahieu et al. **Thin Solid Films, 515 (2006), pp. 1229-1249.**



Schematic of extended structure zone model (ESZM).

S. Mahieu et al. **Thin Solid Films, 515 (2006), pp. 1229-1249.**

Structure / µstructure/ Morphology

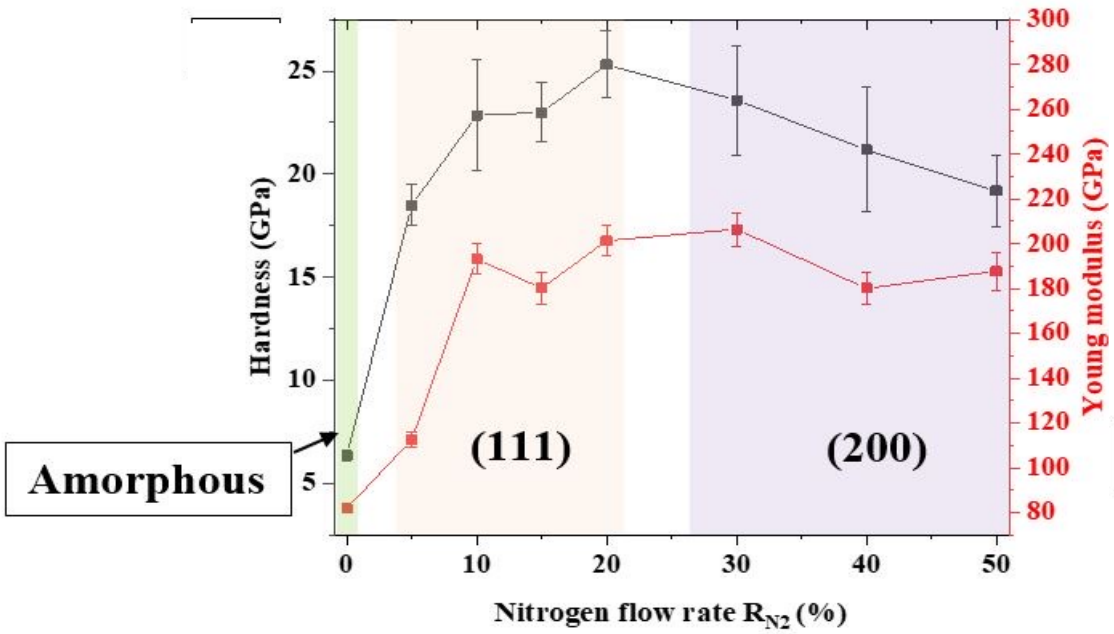


Ta-Zr-Hf-Ti-(Al) (-N)

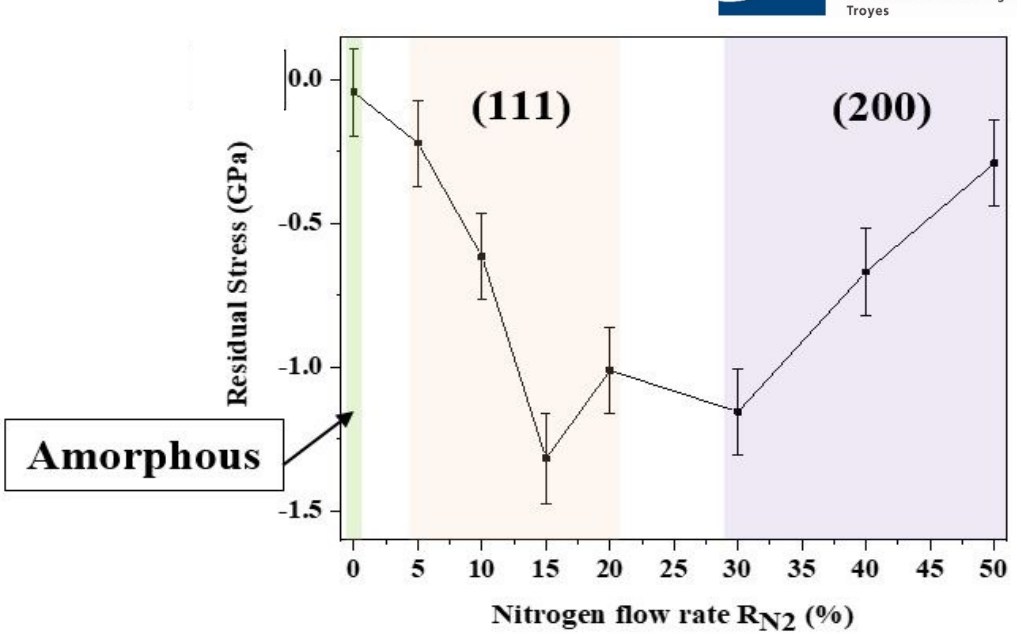
- TEM results are consistent with XRD patterns above.

Mechanical properties.

Ta-Zr-Hf-Ti-(Al) (-N) high entropy films



Hardness and Young's modulus



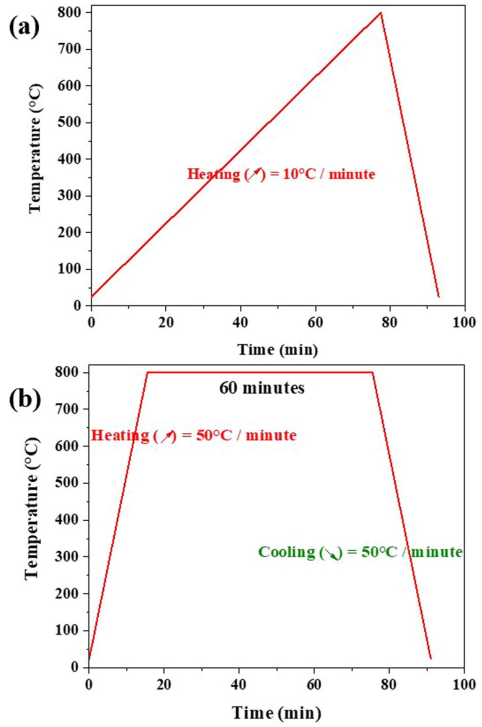
Residual stress of Ta-Zr-Hf-Ti-(Al)-N films as a function of R_{N2}.

- Hardness and Young's modulus are in the ranges 6.4 GPa to 25.3 GPa and 81.9 GPa to 205.5 GPa, respectively.
- When the nitrogen flow increased up to 20 %, the hardness of the deposited films increased due to the formation of strong Metal-Nitrogen bounds as well as a significant decrease of the mean grain size.
- The residual stress increase could be due to the evolution of bombardment energy. As R_{N2} continues to increase, a relaxation of the residual stress occurs because of “amorphization trend”.

High temperature oxidation resistance.

ATG-thermogravimetric analysis

Oxidation test protocols in a simulated dry air atmosphere: 80% N_2 / 20% O_2



- **Kinetic constant** (Kp) : "speed" of the reaction at a given temperature ($g^2/cm^4.h$)
- **Activation Energy** (Ea) : energy required to initiate the reaction (kJ/mol)

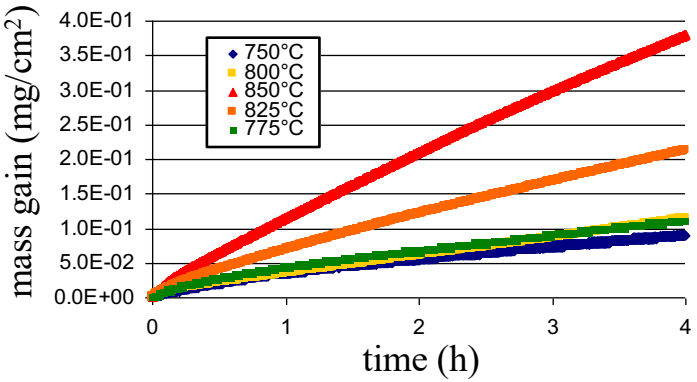
Parabolic curves

↕

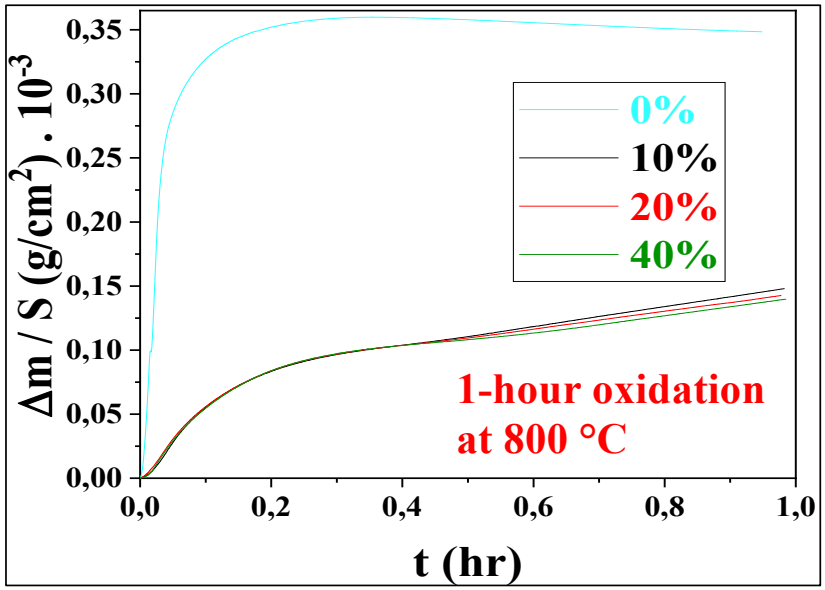
Limited, controlled reaction by the diffusion of species

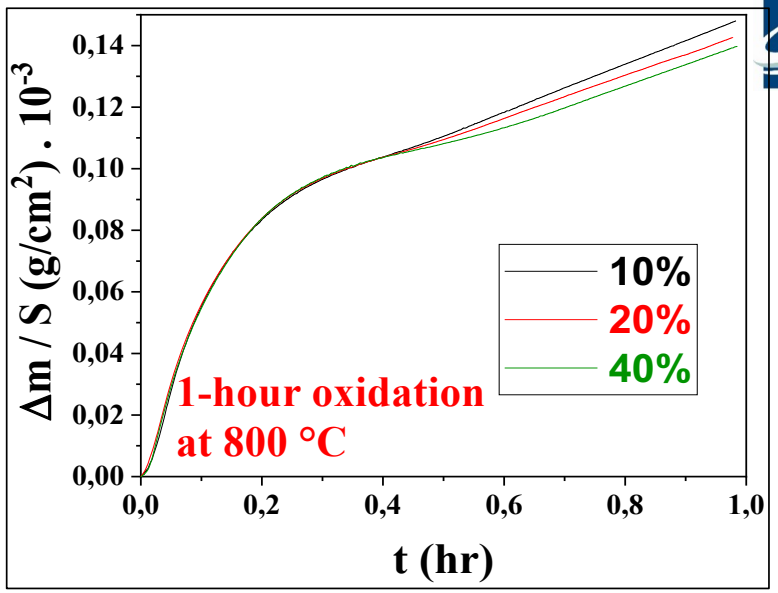
$$\left(\frac{\Delta m}{S}\right)^2 = Kp.t$$

$$Kp = \exp\left(\frac{-Ea}{R.T}\right)$$

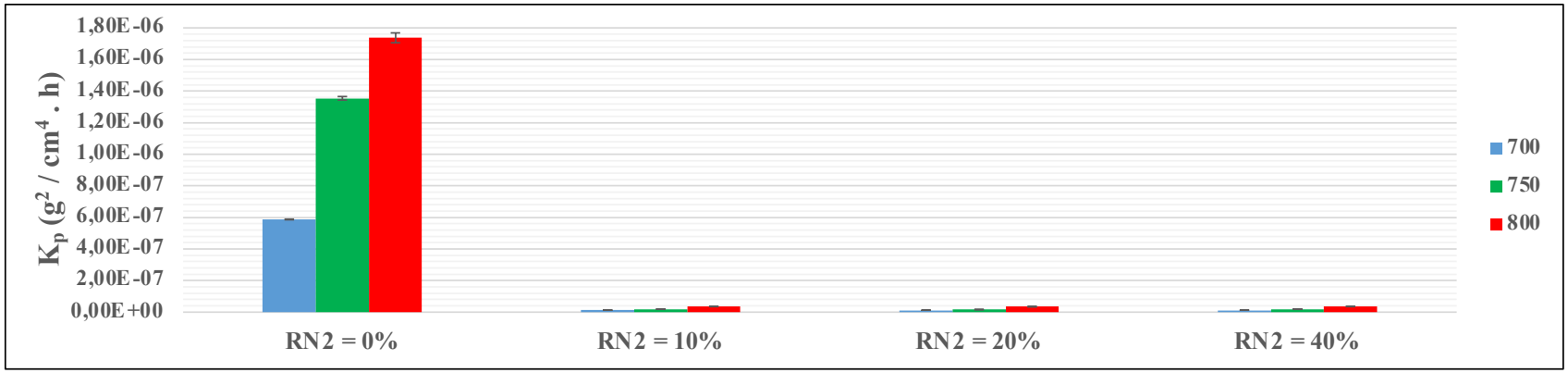


High temperature oxidation resistance. Ta-Zr-Hf-Ti-(Al) (-N)





- By adding the nitrogen into the films, strong N – Metal bounds were formed leading to oxidation resistance improvement.

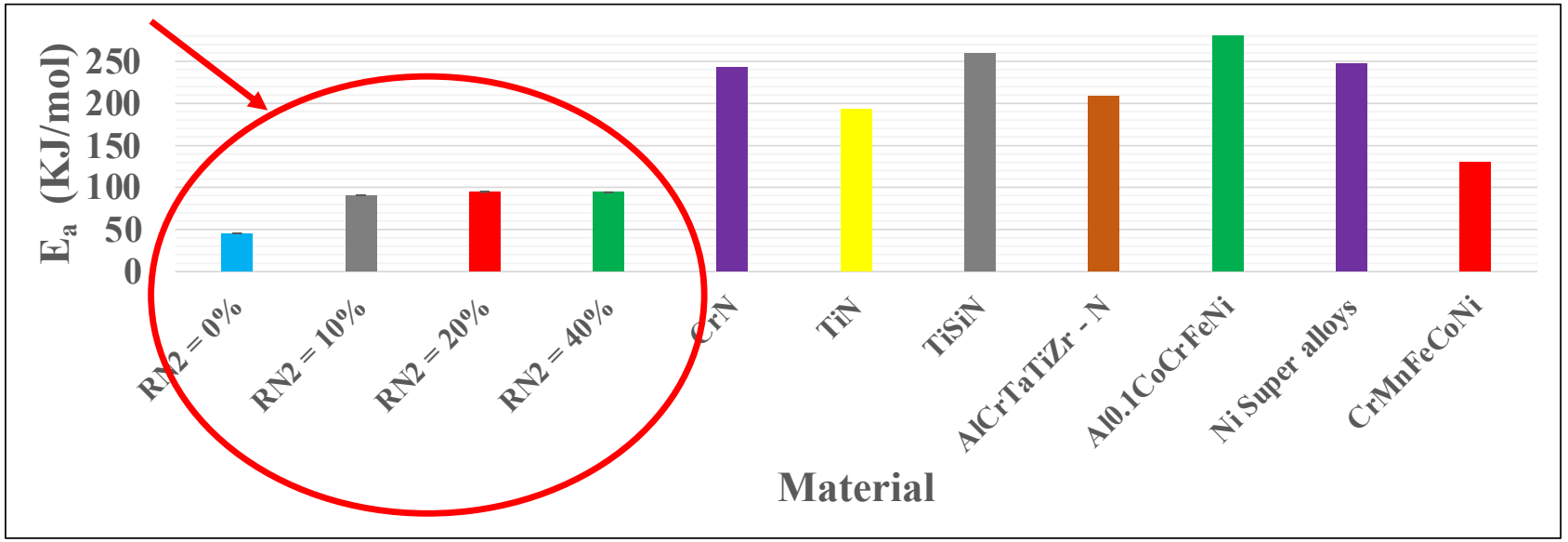


$$\left(\frac{\Delta m}{S}\right)^2 = K_p \cdot t$$

Kinetic constant Kp of $(AlTiZrHfTa)_{1-x}N_x$ films obtained at R_{N2} = 0 %, 10 %, 20 % and 40 %.

High temperature oxidation resistance.

Ta-Zr-Hf-Ti-(Al) (-N)

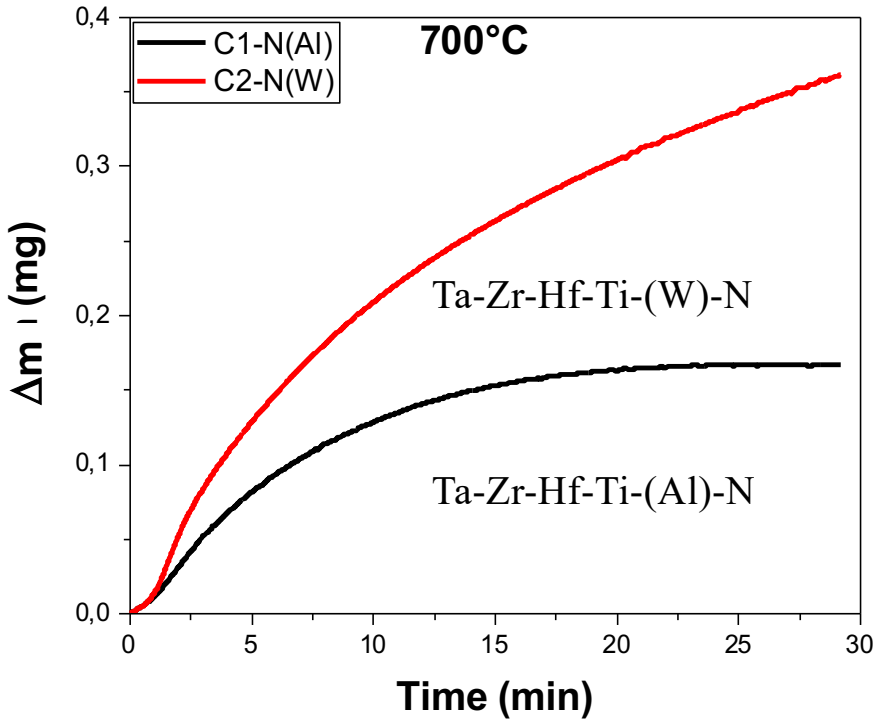


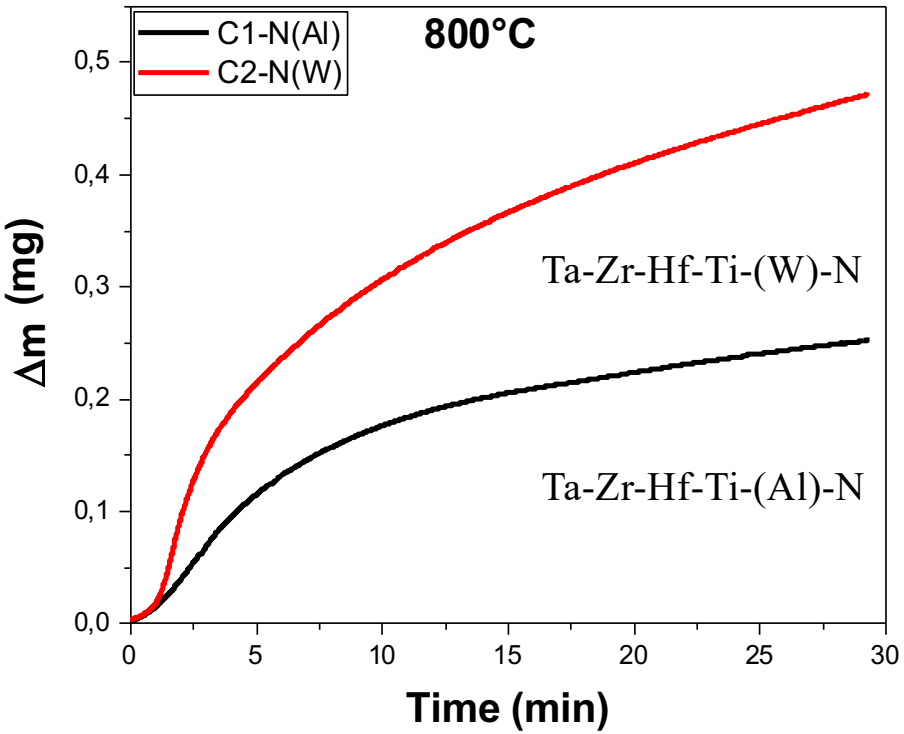
Activation energy Ea of Ta-Zr-Hf-Ti-(Al) (-N) for R_{N2} = 0%, 10%, 20% and 40% and different investigated coatings.

- Oxidation resistance of Ta-Zr-Hf-Ti-(Al) (-N) nitrides films is better than that of metallic material, however the level of resistance remains lower compared to other high entropy films (literature).
- It can be due to several factors:
  - Volumetric expansion mismatch (HEA structure – oxide).
  - Lack of formation of passive protecting oxide on the film surfaces (B. Gorr, S et al. **Adv. Eng. Mater., vol. 23, no 5, p. 2001047, 2021.)**

High temperature oxidation resistance.

Comparison Ta-Zr-Hf-Ti-(Al)-N / Ta-Zr-Hf-Ti-(W)-N





Oxidation resistance is better for coatings containing aluminum rather than tungsten.

This phenomenon is likely due to the volatile nature of tungsten oxides. The oxide layer, in this case, is therefore more porous and does not constitute an efficient barrier to oxygen diffusion.

- XRD, TEM and SEM analyzes reveal a transition from amorphous to an FCC single phase by adding nitrogen.

- The metallic film has a glassy morphology whereas crystalline nitride films have a compact / columnar morphology.

- The best compromise in terms of properties and deposition rate is obtained for the low nitrogen contents in the gas mixture

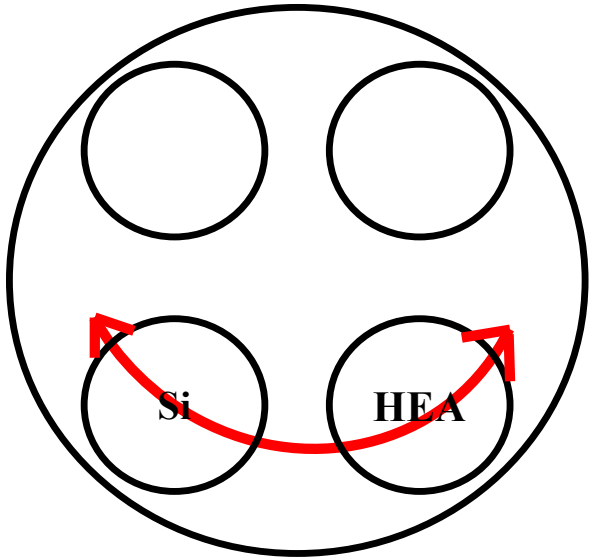
- A relatively low oxidation resistance is measured compared to the coatings reported in literature.

- The oxidation resistance can be further improved, either by adding new chemical element (eg. Si) or by surface coating (Al_2O_3).

Effect of Si addition on the oxidation resistance.

Magnetron sputtering.

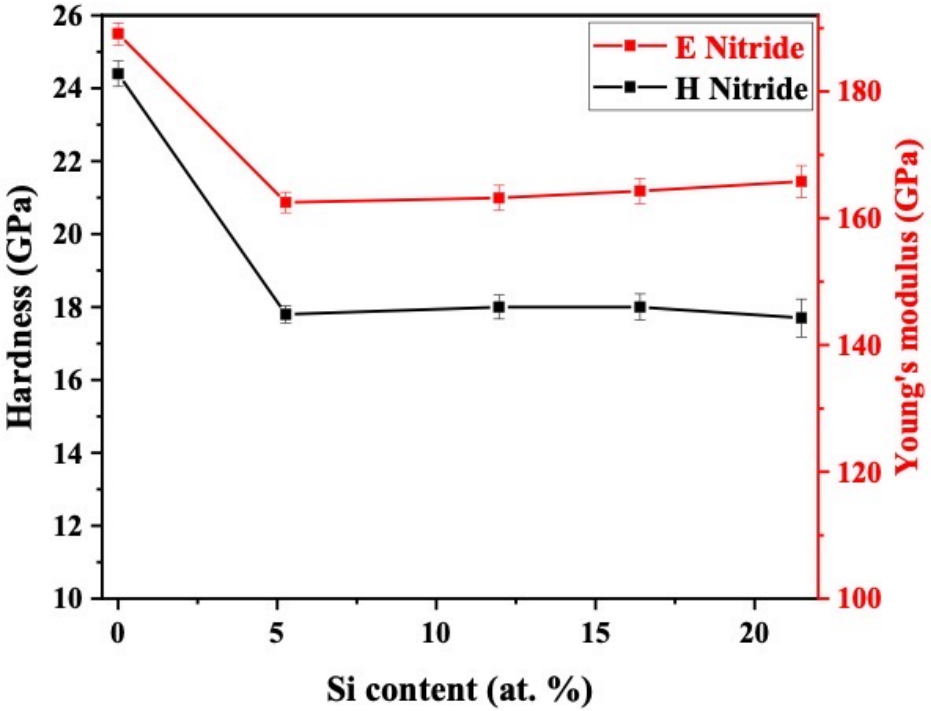
Ta-Zr-Hf-Ti-Al(-Si)-N



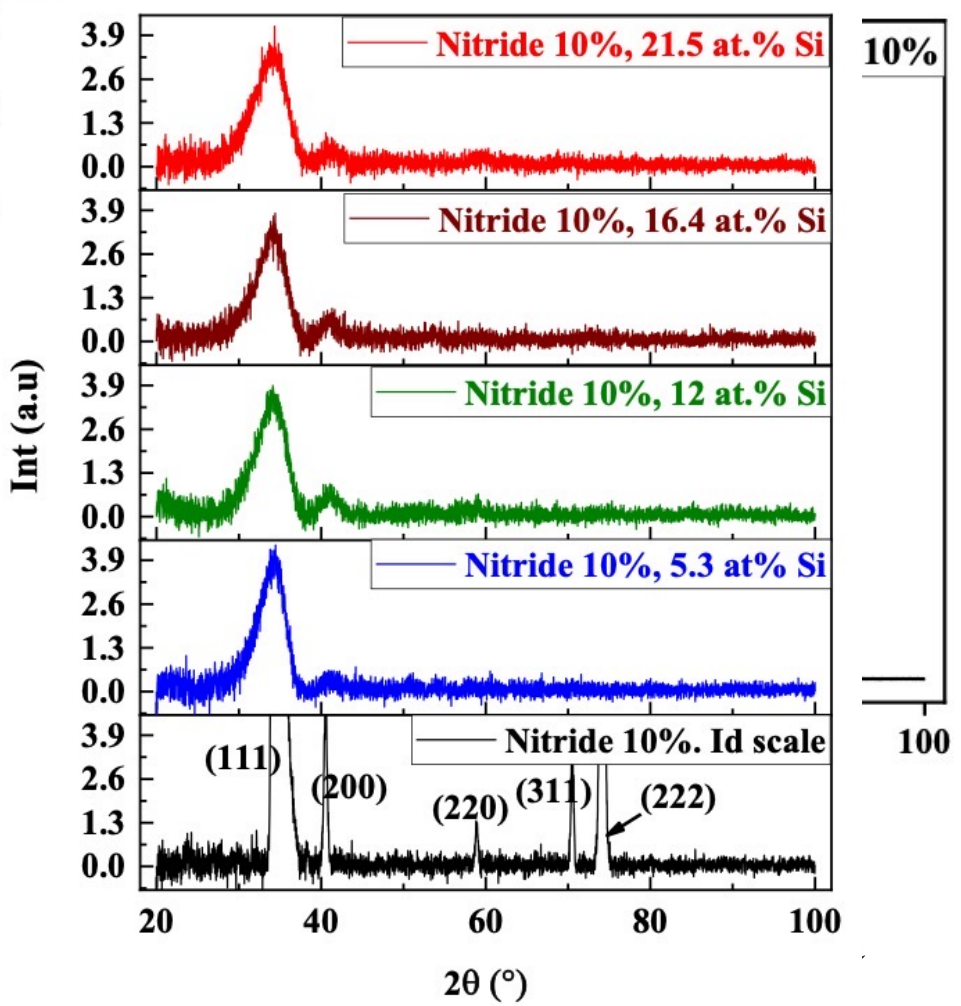
- Equi-atomic target: Al/W, Ti, Zr, Hf and Ta.
- Si target.
- Target – substrate distance = 6 cm.

Deposition parameters					
I, HEA (A)	I, Si (A)	Si (at.%)	P (Pa)	$R_{N2}=\Phi_{N2}/\Phi_{N2}+\Phi_{Ar}$	Mode / Rpm
1	0	0	1	**10 %**	Scanning / 2 Rpm
1	0,1	5,3	1	**10 %**	Scanning / 2 Rpm
1	0,2	12	1	**10 %**	Scanning / 2 Rpm
1	0,3	16,5	1	**10 %**	Scanning / 2 Rpm
1	0,4	21,4	1	**10 %**	Scanning / 2 Rpm

Effect of Si addition on structure and hardness



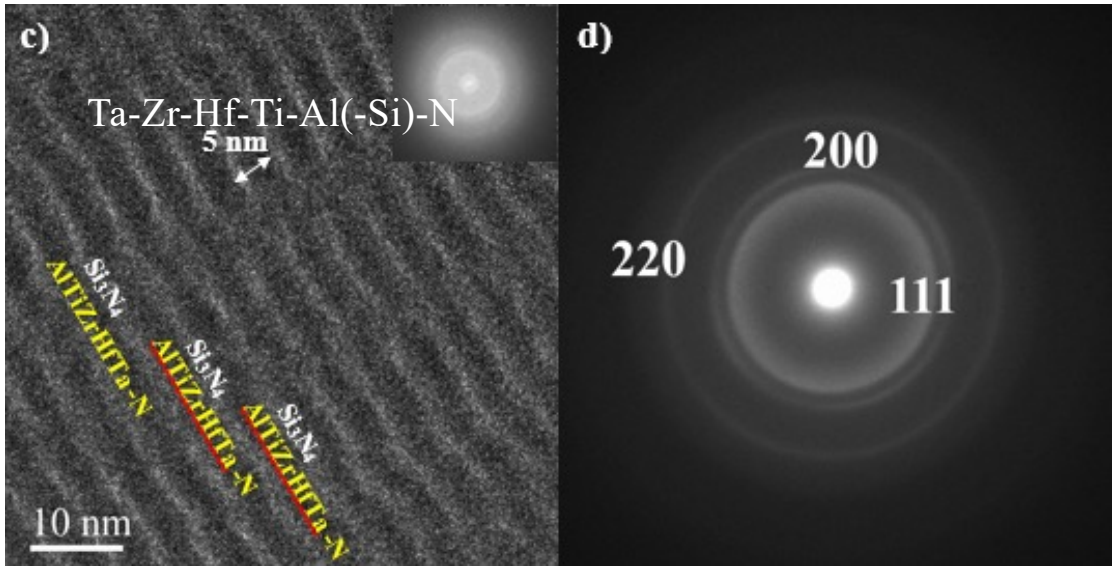
Hardness and Young's modulus of (AlTiZrHfTa)-Si_x-N, R_{N2} = 10 %, films at various Si content (at. %).



- H decreases from 24 GPa to 18 GPa and E also decreases from 188 GPa to about 162 GPa.
- Addition of Si → broader peaks + lower intensities compared to those of undoped nitride.

Effect of Si addition on the oxidation resistance.

Ta-Zr-Hf-Ti-Al(-Si)-N

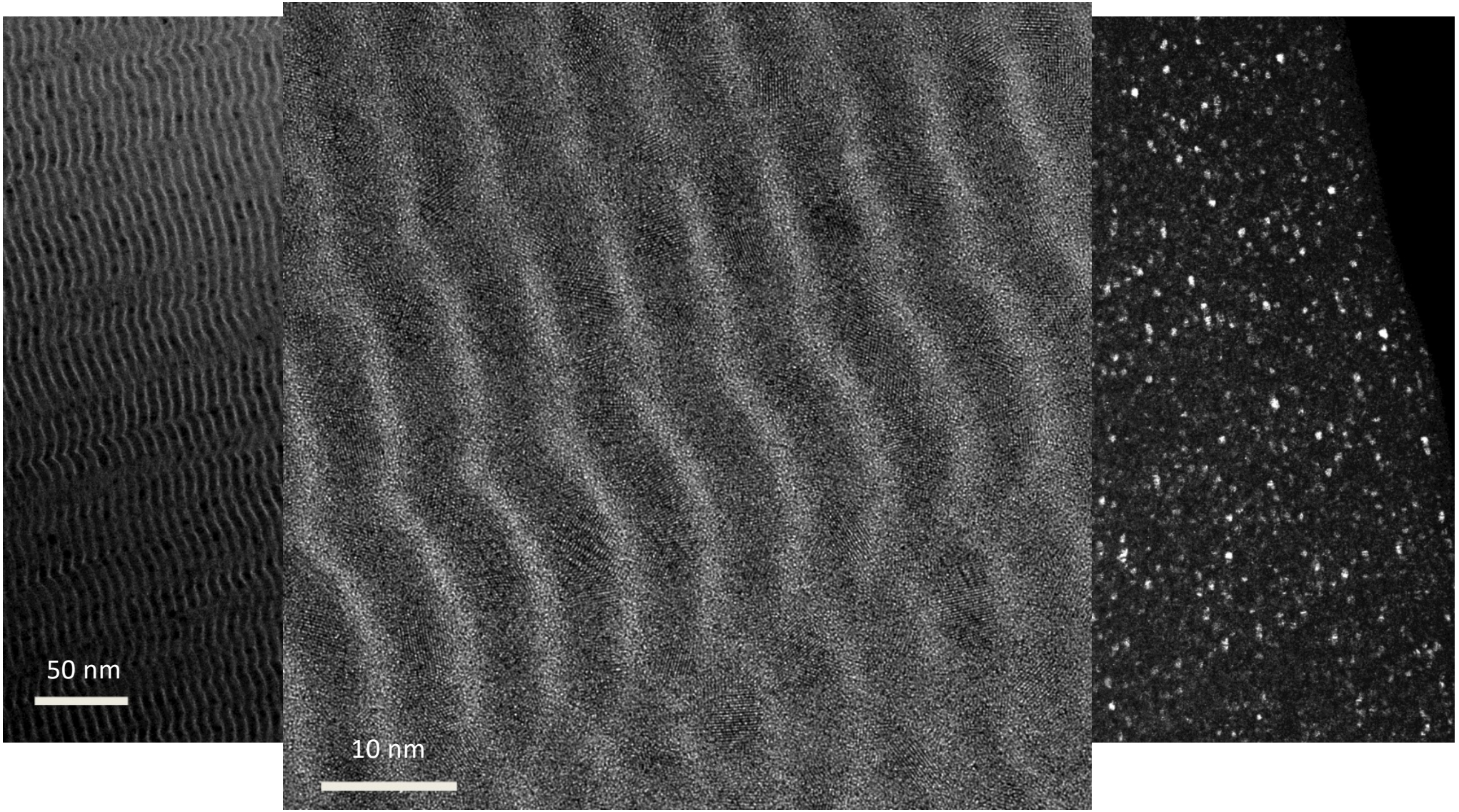


HRTEM micrograph and inserted FFT. (d) SAED pattern of $(AlTiZrHfTa)_{1-x}\ N_x$ film at R_{N2} = 10 % doped with 12 at.% Si.

Si addition = compacity increases + deposition of an obvious nano-layered configuration.

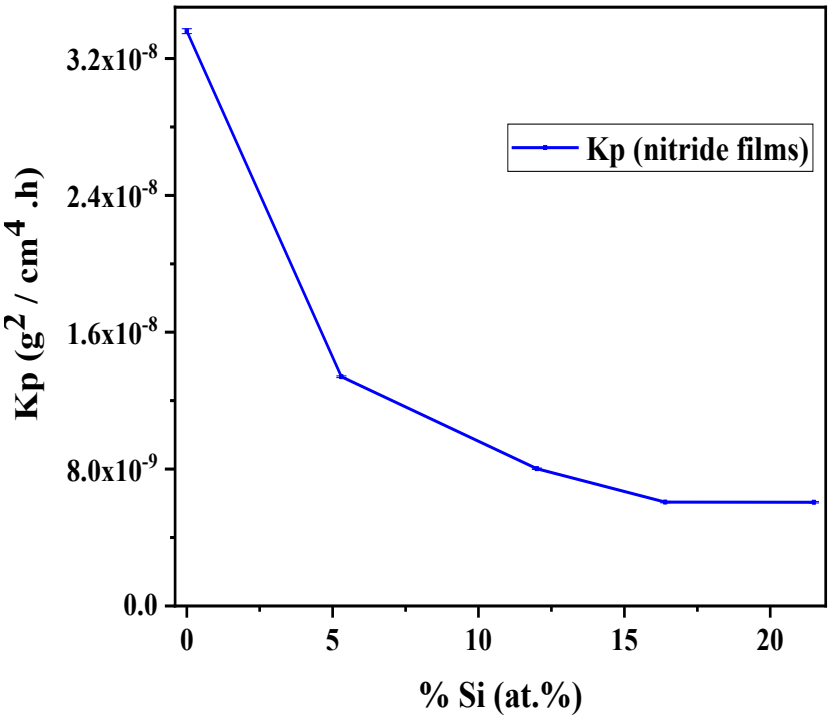
Effect of Si addition on the oxidation resistance.

Ta-Zr-Hf-Ti-W(-Si)-N

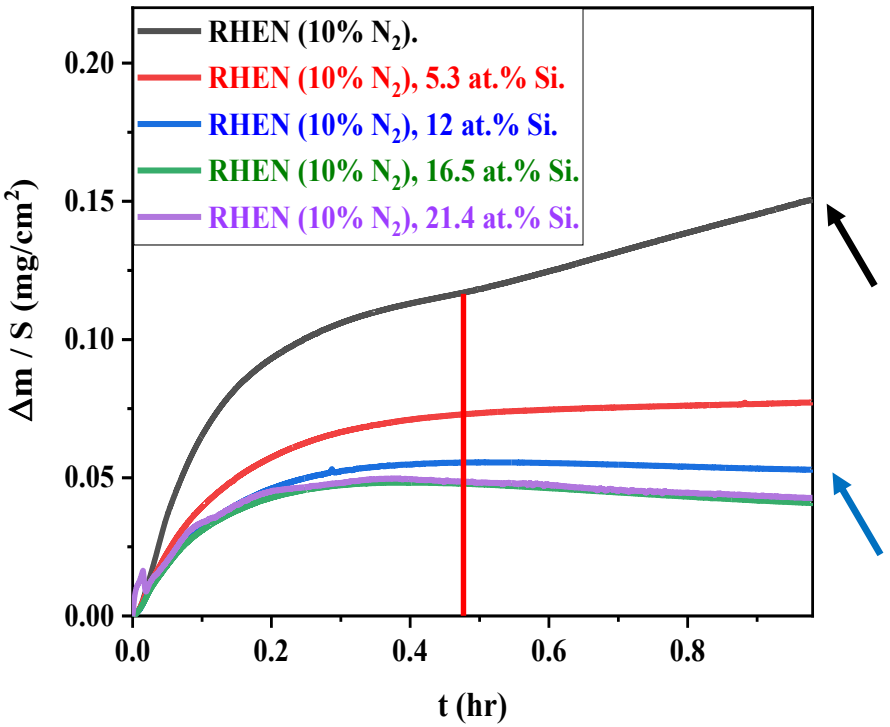


Effect of Si addition on the oxidation resistance.

Ta-Zr-Hf-Ti-Al(-Si)-N



Kinetic constant K_p of Ta-Zr-Hf-Ti-Al(-Si)-N nitride films obtained at (R_{N2} = 10 %) at 800 °C at various Si-target current.



Oxidation kinetic curves of Ta-Zr-Hf-Ti-Al(-Si)-N nitride films obtained at (R_{N2} = 10 %) at 800 °C

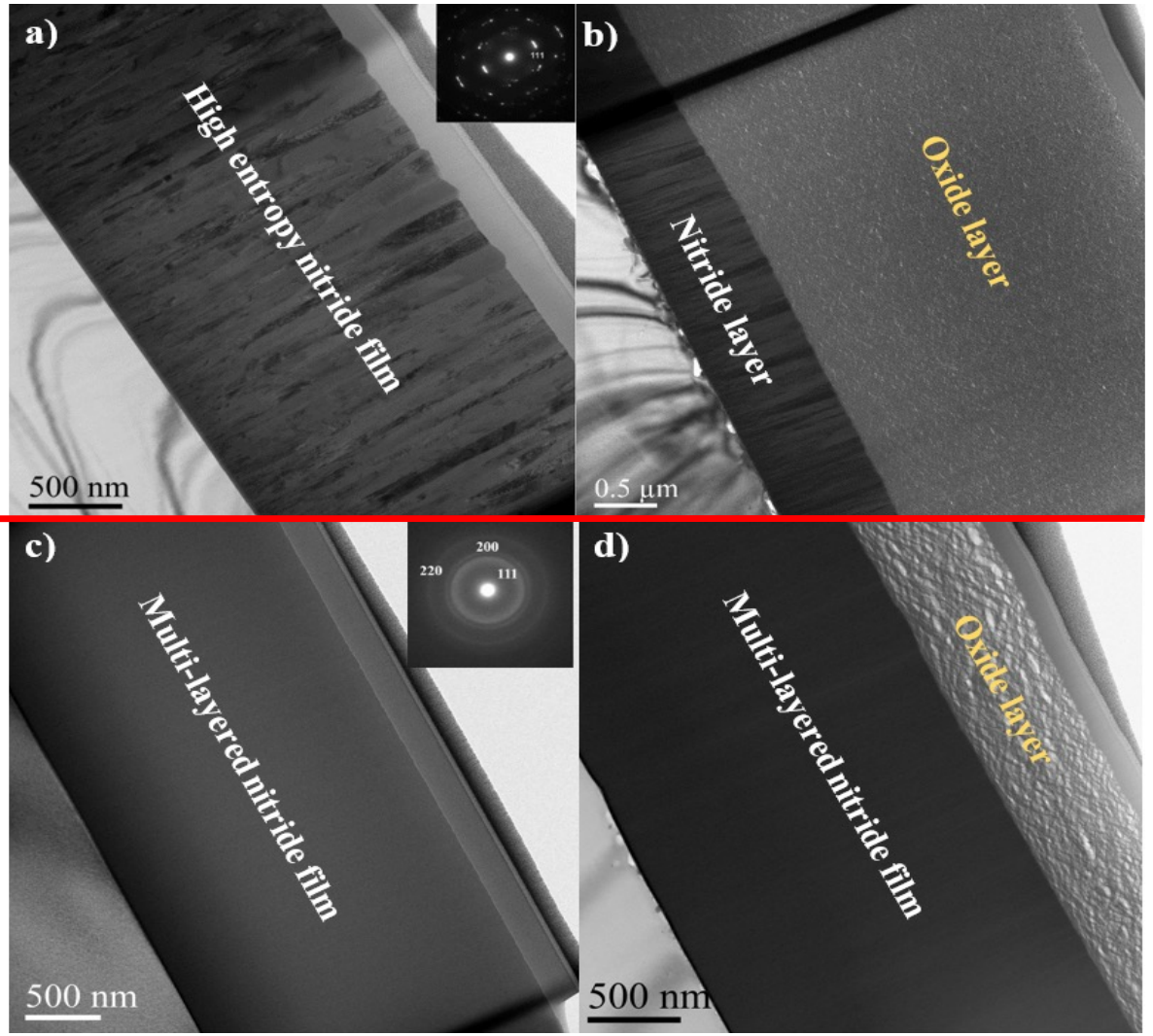
- The addition of Si reduces the Kp values, resulting from the formation of nano-multilayered configuration (FCC **Ta-Zr-Hf-Ti-Al(-Si)-N** nanolayer and amorphous **(Si-N)** nanolayer)

Effect of Si addition on the oxidation resistance.

Ta-Zr-Hf-Ti-Al(-Si)-N

Si-free nitride film

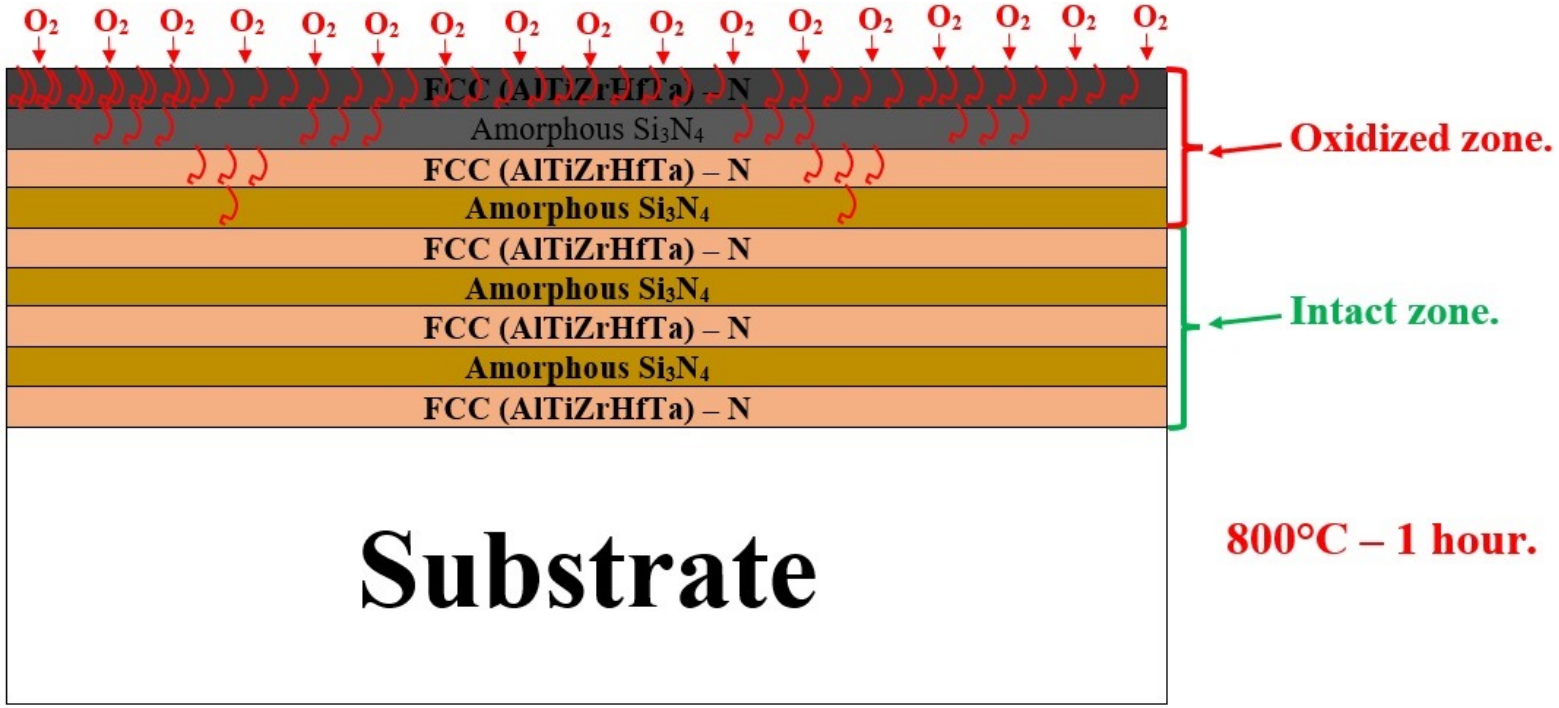
Si doped nitride film



BF TEM micrograph of intact nitride film at R_{N2}=10% and Si-doped (12 at.%) film before and after 1hour oxidation at 800°C.

Effect of Si addition on the oxidation resistance.

Ta-Zr-Hf-Ti-Al(-Si)-N / Towards Nanocomposite material



Nitride film at R_{N2}=10% and Si-doped (12 at.%) film before and after 1hour oxidation at 800°C.

CONCLUSION:

- It's relatively easy to obtain FCC single phased High Entropy Alloys Films by conventional magnetron sputtering of one alloying target. Maximum H = 26 GPa and E_R = 206 GPa are measured

- The increase of Si content in the film leads to decrease significantly the kinetic constant Kp, associated with an oxidation resistance improvement of the Si-doped films.

Bibliography, references

[1]: Y. Zhang, X.-H. Yan, W.-B. Liao, et K. Zhao, « **Effects of Nitrogen Content on the Structure and Mechanical Properties of (Al0.5CrFeNiTi0.25)Nx High-Entropy Films by Reactive Sputtering** », Entropy, vol. 20, no 9, Art. no 9, sept. 2018, doi: 10.3390/e20090624.

[2]: EJ. Yeh, S. Chen, S. Lin, J. Gan, T. Chin, T. Shun, C. Tsau, S. Chang **Nanostructured high-entropy alloys with multiple principal elements: novel alloy design concepts and outcomes**
Adv. Eng. Mater., 6 (2004), pp. 299-303.

[3]: H.-W. Chang, P.-K. Huang, A. Davison, J.-W. Yeh, C.-H. Tsau, C.-C. YangNitride films deposited from an equimolar Al–Cr–Mo–Si–Ti alloy target by reactive direct current magnetron sputtering
Thin Solid Films, 516 (2008), pp. 6402-6408

[4]: C.-H. Lai, S.-J. Lin, J.-W. Yeh, S.-Y. Chang **Preparation and characterization of AlCrTaTiZr multi-element nitride coatings**. Surf. Coat. Technol., 201 (2006), pp. 3275-3280.

[5]: S. Mahieu, P. Ghekiere, D. Depla, R. De Gryse **Biaxial alignment in sputter deposited thin films**
Thin Solid Films, 515 (2006), pp. 1229-1249

[6] S. Achache, A. Alhussein, B. Guelorget, R. Salut, M. François, et F. Sanchette**, « Effect of oxygen addition on microstructure and mechanical properties of quaternary TNTZ superelastic thin films obtained by magnetron sputtering** », Mater. Chem. Phys., vol. 217, p. 262-269, sept. 2018, doi: 10.1016/j.matchemphys.2018.06.066.

Bibliography, references

[7]: M. El Garah, S. Achache, A. Michau, F. Schuster, et F. Sanchette, « **Structural and mechanical properties of AlTiTaZr(N) medium entropy films (MEF) obtained by DC magnetron sputtering in dynamic mode** », Surf. Coat. Technol., vol. 396, p. 125941, août 2020, doi: 10.1016/j.surfcoat.2020.125941.

[8]: S. Li et T. Yamaguchi, « **High-temperature oxidation behavior of laser-cladded refractory NiSi0.5CrCoMoNb0.75 high-entropy coating** », J. Mater. Res. Technol., vol. 17, p. 1616-1627, mars 2022, doi: 10.1016/j.jmrt.2022.01.115.

[9]: B. Gorr, S. Schellert, F. Müller, H.-J. Christ, A. Kauffmann, et M. Heilmaier, « **Current Status of Research on the Oxidation Behavior of Refractory High Entropy Alloys** », Adv. Eng. Mater., vol. 23, no 5, p. 2001047, 2021, doi: 10.1002/adem.202001047.

[10]: https://www.heroal.de/Website-content/Service/oberflaechenbeschichtung/heroal-hwr-pulverbeschichtung_370x250-7.jpg

[11]: Wojciechowski, Paweł, et Mikołaj Lewandowski. « **Iron Nitride Thin Films: Growth, Structure, and Properties** ». Crystal Growth & Design 22, no 7 (6 juillet 2022): 4618-39. https://doi.org/10.1021/acs.cgd.1c01528.

[12] P. Eh. Hovsepian, D. B. Lewis, et W.-D. Münz, « **Recent progress in large scale manufacturing of multilayer/superlattice hard coatings** », Surf. Coat. Technol., vol. 133-134, p. 166-175, nov. 2000, doi: 10.1016/S0257-8972(00)00959-2.

Bibliography, references

[13] M. Tomlinson, S. B. Lyon, P. Hovsepian, et W.-D. Munz, « **Corrosion performance of CrN/NbN superlattice coatings deposited by the combined cathodic arc/unbalanced magnetron technique** », Vacuum, vol. 53, no 1, p. 117-121, mai 1999, doi: 10.1016/S0042-207X(98)00405-9.

[14] W. Zhang et al., « **Improved corrosion resistance of reactive gas pulse sputtered (TiTaNbZrNi)N high entropy alloy coatings with a hybrid architecture of multilayered and compositionally graded structures** », J. Nucl. Mater., vol. 543, p. 152558, janv. 2021, doi: 10.1016/j.jnucmat.2020.152558.

[15] D. E. Touaibia et al., « **Oxidation Resistance and Mechanical Properties of Altizrhfta(-N) High Entropy Films Deposited by Reactive Magnetron Sputtering** ». Rochester, NY, 30 septembre 2022. doi: 10.2139/ssrn.4234157.

Thank you